Eur J Nucl Med Mol Imaging (2014) 41:476–485
DOI 10.1007/s00259-013-2563-z

ORIGINAL ARTICLE

Direct in vitro and in vivo comparison of ^{161}Tb and ^{177}Lu using a tumour-targeting folate conjugate

Cristina Müller · Josefine Reber · Stephanie Haller · Holger Dorrer · Peter Bernhardt · Konstantin Zhernosekov · Andreas Türler · Roger Schibli

Received: 25 June 2013 / Accepted: 27 August 2013 / Published online: 8 October 2013

Abstract
Purpose The radiolanthanide ^{161}Tb ($T_{1/2}$=6.90 days, $E\beta^-_{av}$=154 keV) was recently proposed as a potential alternative to ^{177}Lu ($T_{1/2}$=6.71 days, $E\beta^-_{av}$=134 keV) due to similar physical decay characteristics but additional conversion and Auger electrons that may enhance the therapeutic efficacy. The goal of this study was to compare ^{161}Tb and ^{177}Lu in vitro and in vivo using a tumour-targeted DOTA-folate conjugate (cm09).

Methods ^{161}Tb-cm09 and ^{177}Lu-cm09 were tested in vitro on folate receptor (FR)-positive KB and IGROV-1 cancer cells using a 3-(4,5-dimethylthiazol-2-yl)-2,5-diphenyltetrazolium bromide (MTT) viability assay. In vivo ^{161}Tb-cm09 and ^{177}Lu-cm09 (10 MBq, 0.5 nmol) were investigated in two different tumour mouse models with regard to the biodistribution, the possibility for single photon emission computed tomography (SPECT) imaging and the antitumour efficacy. Potentially undesired side effects were monitored over 6 months by determination of plasma parameters and examination of kidney function with quantitative SPECT using ^{99m}Tc-dimercaptosuccinic acid (DMSA).
Results To obtain half-maximal inhibition of tumour cell viability a 4.5-fold (KB) and 1.7-fold (IGROV-1) lower radioactivity concentration was required for ^{161}Tb-cm09 (IC_{50} ~0.014 MBq/ml and ~2.53 MBq/ml) compared to ^{177}Lu-cm09 (IC_{50} ~0.063 MBq/ml and ~4.52 MBq/ml). SPECT imaging visualized tumours of mice with both radioconjugates. However, in therapy studies ^{161}Tb-cm09 reduced tumour growth more efficiently than ^{177}Lu-cm09. These findings were in line with the higher absorbed tumour dose for ^{161}Tb-cm09 (3.3 Gy/MBq) compared to ^{177}Lu-cm09 (2.4 Gy/MBq). None of the monitored parameters indicated signs of impaired kidney function over the whole time period of investigation after injection of the radiofolates.
Conclusion Compared to ^{177}Lu-cm09 we demonstrated equal imaging features for ^{161}Tb-cm09 but an increased therapeutic efficacy for ^{161}Tb-cm09 in both tumour cell lines in vitro and in vivo. Further preclinical studies using other tumour-targeting radioconjugates are clearly necessary to draw final conclusions about the future clinical perspectives of ^{161}Tb.

Keywords ^{161}Tb · ^{177}Lu · Therapy · Folate · Folate receptor · Cancer

Electronic supplementary material The online version of this article (doi:10.1007/s00259-013-2563-z) contains supplementary material, which is available to authorized users.

C. Müller (✉) · J. Reber · S. Haller · R. Schibli (✉)
Center for Radiopharmaceutical Sciences ETH-PSI-USZ, Paul Scherrer Institute, Villigen-PSI, Switzerland
e-mail: cristina.mueller@psi.ch
e-mail: roger.schibli@psi.ch

H. Dorrer · K. Zhernosekov · A. Türler
Laboratory of Radiochemistry and Environmental Chemistry, Paul Scherrer Institute, Villigen-PSI, Switzerland

H. Dorrer · A. Türler
Laboratory of Radiochemistry and Environmental Chemistry, Department of Chemistry and Biochemistry, University of Bern, Bern, Switzerland

P. Bernhardt
Department of Radiation Physics, The Sahlgrenska Academy, University of Gothenburg, Gothenburg, Sweden

P. Bernhardt
Department of Medical Physics and Medical Bioengeneering, Sahlgrenska University Hospital, Gothenburg, Sweden

R. Schibli
Department of Chemistry and Applied Biosciences, ETH Zurich, Zurich, Switzerland

Introduction

The concept of peptide receptor radionuclide therapy (PRRT) using radiolabelled somatostatin analogues (e.g. DOTATATE and DOTATOC) proved its potential for the management of patients with inoperable or metastasized neuroendocrine tumours over many years [1, 2]. The first particle-emitting radioisotope used for PRRT was ^{90}Y, which decays with a half-life of 2.67 days by emission of β^--particles of a relatively high energy ($E\beta^-_{av}$=934 keV) [3]. In spite of the encouraging results obtained with PRRT, it has occasionally resulted in severe nephrotoxicity [4, 5]. By introduction of the radiolanthanide ^{177}Lu ($T_{1/2}$=6.71 days, $E\beta^-_{av}$=134 keV) as an alternative to ^{90}Y [6, 7] undesired side effects to the kidneys became less problematic due to its softer β^--energy spectrum compared to ^{90}Y [8].

Herein, we propose another radiolanthanide, ^{161}Tb, as an alternative isotope for targeted radionuclide therapy [9–11]. ^{161}Tb decays with a half-life of 6.90 days by emission of low-energy β^--particles ($E\beta^-_{av}$=154 keV) [9]. Similar to ^{177}Lu which emits gamma radiation of energies suitable for single photon emission computed tomography (SPECT) imaging, the β^--decay of ^{161}Tb is accompanied by emission of gamma rays of energies ($E\gamma$=25.7 keV, 48.9 keV, 74.6 keV) that allow its use for SPECT as well. Importantly, ^{161}Tb emits a significant number of conversion and Auger electrons of energies ≤ 40 keV (~12.12 e^-, ~36.1 keV per decay) compared to ^{177}Lu whose decay is accompanied by only a negligible number of electrons (~1.11 e^-, ~1.0 keV per decay) in the same energy window (Table 1) [12]. This additional energy release of ^{161}Tb is even higher than for commonly employed Auger and conversion electron emitters such as ^{125}I (~23.95 e^-, ~19.2 keV per decay) and ^{123}I (~13.71 e^-, ~7.2 keV per decay) or ^{111}In (~7.43 e^-, ~6.9 keV per decay) and ^{67}Ga (~4.96 e^-, ~6.6 keV per decay) [12]. Since both ^{177}Lu and ^{161}Tb belong to the group of lanthanides, the same (radio)chemistry may be applied and hence the formation of highly stable complexes of ^{177}Lu upon coordination by a DOTA chelator is also possible for ^{161}Tb [9]. Recently, we have implemented routine production of ^{161}Tb [9] at the Paul Scherrer Institute. The radiopharmaceutical utility of this and other Tb radioisotopes has been demonstrated in a recent proof-of-concept study [11].

Table 1 Comparison of the production and decay properties of ^{161}Tb and ^{177}Lu

Isotope	^{161}Tb		^{177}Lu	
Production	^{160}Gd(n,γ)^{161}Gd→ ^{161}Tb [9]		(1) ^{176}Lu(n,γ)^{177}Lu [23, 24] (2) ^{176}Yb(n,γ)^{177}Yb→^{177}Lu [25]	
Half-life	6.90 days		6.71 days	
$E\beta^-_{av}$ (intensity)	154 keV	(1.00)	134 keV	(1.00)
Eγ (intensity)	25.7 keV	(0.23)	112.9 keV	(0.062)
	48.9 keV	(0.17)	208.4 keV	(0.104)
	74.6 keV	(0.10)		
Conversion and Auger electrons (intensity) [12]	0–0.1 keV	(0.72)	0–0.1 keV	(0.27)
	0.1–1 keV	(7.38)	0.1–1 keV	(0.55)
	1–10 keV	(3.03)	1–10 keV	(0.30)
	10–20 keV	(0.42)	10–20 keV	
	20–30 keV	(0.18)	20–30 keV	
	30–40 keV	(0.39)	30–40 keV	
	0–40 keV	(12.13)	0–40 keV	(1.11)

The aim of this study was to compare ^{161}Tb with ^{177}Lu and to evaluate potentially different features in terms of SPECT imaging and in vitro and in vivo antitumour efficacy. For this purpose we employed a recently developed DOTA-folate conjugate (cm09) which previously proved favourable in vitro and in vivo properties [13]. Due to the improved tissue distribution profile of ^{177}Lu-cm09 compared to conventional folate radioconjugates it could also be used for preclinical therapy experiments with tumour-bearing mice [11, 13]. Therefore, the folate conjugate (cm09) appeared to be an excellent tool to investigate ^{161}Tb and compare it with ^{177}Lu (Fig. 1).

In vitro ^{161}Tb-cm09 and ^{177}Lu-cm09 were investigated with regard to their effects on the viability of folate receptor (FR)-positive cancer cells upon exposure to variable radioactivity concentrations. In vivo therapy studies were performed with ^{161}Tb-cm09 and ^{177}Lu-cm09 for direct comparison in established tumour mouse models. For this purpose we used KB (human cervical carcinoma) and IGROV-1 (human ovarian carcinoma) tumour xenografts. The two radiolanthanides ^{161}Tb and ^{177}Lu were also compared with regard to their potential for preclinical SPECT imaging, which we investigated by phantom studies and by in vivo scans in tumour-bearing mice.

Materials and methods

Radioisotopes

No-carrier-added (n.c.a.) ^{161}Tb was produced by irradiation of enriched ^{160}Gd targets for 3 weeks at the spallation-induced neutron source (SINQ) at PSI (Villigen-PSI, Switzerland) or by irradiation for 1 week at the high-flux nuclear reactor of ILL (Grenoble, France) [11]. Isolation and formulation of high concentrated $^{161}TbCl_3$ in 0.05 M HCl (2–3 GBq/100 μl) was performed according to the procedure previously reported by Lehenberger et al. [9]. $^{177}LuCl_3$ (in 0.04 M HCl) was obtained from Isotope Technologies Garching GmbH (ITG GmbH, Munich, Germany) at an activity concentration of 1 GBq/100 μl. The exact amount of radioactivity of these radionuclides was measured with a calibrated N-type high-purity germanium (HPGe) coaxial detector (EURISYS MESURES) and the Ortec InterWinner 5.0 software.

Radiofolate synthesis

Depending on the activity concentration of the radioisotopes, x μl of a $^{161}TbCl_3$ or $^{177}LuCl_3$ solution corresponding to

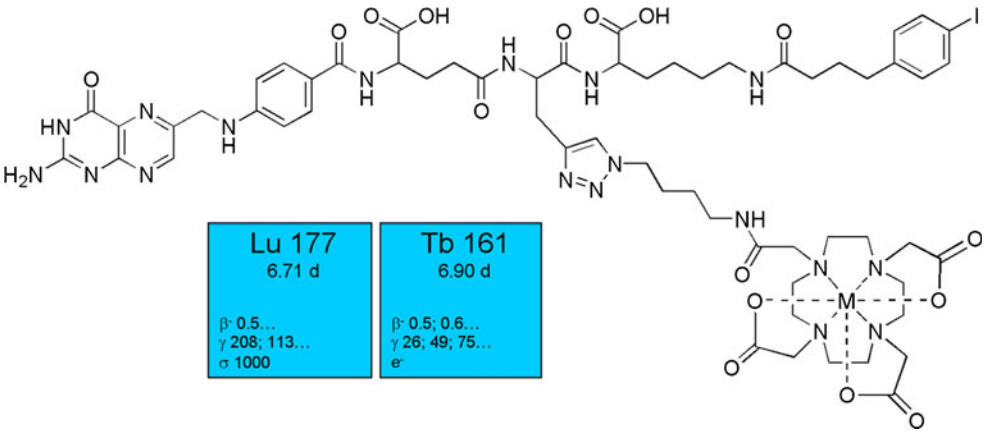

Fig. 1 Chemical structure of the folate radioconjugate (M-cm09) comprising folic acid as the FR-targeting ligand, an albumin-binding entity to enhance the blood circulation time and a DOTA chelator for stable coordination of the radioisotope (M=^{161}Tb, ^{177}Lu)

300 MBq was added to a mixture of cm09 (10 μl, 10^{-3} M), 0.05 M HCl (100-x μl) and 0.5 M sodium acetate (20 μl) to obtain ^{161}Tb-cm09 and ^{177}Lu-cm09 at a specific activity of up to 30 MBq/nmol. The reaction solution was heated for 10 min at 95 °C. After cooling down to room temperature Na-diethylenetriaminepentaacetic acid (Na-DTPA, 10 μl, 5 mM, pH 5) was added for complexation of potential traces of unreacted ^{161}Tb(III) and ^{177}Lu(III), respectively. Quality control was performed by HPLC using a C18 reversed phase column (XTerra MS C18, 5 μm, 15 cm × 4.6 cm, Waters). The mobile phase consisted of Milli-Q water with 0.1 % trifluoroacetic acid (A) and methanol (B) with a linear gradient from 5 % B to 80 % B over 25 min at a flow rate of 1 ml/min.

Cell culture

KB cells (human cervical carcinoma cell line, HeLa subclone; ACC-136) were purchased from the German Collection of Microorganisms and Cell Cultures (DSMZ, Braunschweig, Germany). IGROV-1 cells (human ovarian carcinoma cell line) were a kind gift from Dr. Gerrit Jansen (Department of Rheumatology, VU University Medical Center, Amsterdam, The Netherlands). The cells were cultured as monolayers at 37 °C in a humidified atmosphere containing 5 % CO_2. Both cell lines were grown in folate-free cell culture medium, FFRPMI (modified RPMI, without folic acid, vitamin B_{12} and phenol red, Cell Culture Technologies GmbH, Gravesano/Lugano, Switzerland) supplemented with 10 % heat-inactivated fetal calf serum (FCS, as the only source of folate), L-glutamine and antibiotics (penicillin/streptomycin/fungizone).

In vitro experiments were performed with ^{161}Tb and ^{177}Lu in salt form ($^{161}TbCl_3$ and $^{177}LuCl_3$), with DTPA-coordinated radioisotopes (^{161}Tb-DTPA and ^{177}Lu-DTPA) and with the radiolabelled folate conjugates (^{161}Tb-cm09 and ^{177}Lu-cm09) at the same specific activity (20 MBq/nmol) which was employed for in vivo experiments.

In vitro cell viability assay

Cell viability was assessed using a 3-(4,5-dimethylthiazol-2-yl)-2,5-diphenyltetrazolium bromide (MTT) assay as described by Mosmann [14]. KB cells and IGROV-1 cells (2,500 cells in 200 μl FFRPMI with supplements) were seeded in 96-well plates. After incubation overnight to allow adhesion of the cells, the supernatants were removed and the cells were incubated in 200 μl FFRPMI medium (without supplements) containing ^{161}Tb-cm09 and ^{177}Lu-cm09, respectively (0.0001–10 MBq/ml). Control assays were performed with cells incubated with FFRPMI medium without radioactivity. After 4 h incubation at 37 °C, cells were washed once with 200 μl phosphate-buffered saline (PBS) followed by addition of 200 μl of FFRPMI medium (with supplements) to each well. Cells were grown over 4 days under standard cell culture conditions (37 °C, 5 % CO_2 and high humidity), before addition of MTT reagent (5 mg/ml in PBS, 30 μl per well). The well plates were incubated for an additional 4 h allowing the formation of dark-violet formazan crystals. Upon replacement of the FFRPMI medium by dimethyl sulphoxide (DMSO, 200 μl per well) to dissolve the crystals, determination of the absorbance was carried out at 560 nm using a microplate reader (VICTOR X3, PerkinElmer). To quantify cell viability, the absorbance of the test samples was expressed as percentage of the absorbance of control cell samples which was set to 100 %. Sigmoid inhibition curves were determined and the radioactivity concentration (MBq/ml) which reduced cell viability to 50 % of untreated control cells was indicated as half-maximal inhibitory concentration (IC_{50}) using GraphPad Prism (version 5).

In vivo studies

In vivo experiments were approved by the local veterinarian department and conducted in accordance with the Swiss law on animal protection. Four- to five-week-old female, athymic

nude mice (CD-1 Foxn1/*nu*) were purchased from Charles River Laboratories (Sulzfeld, Germany). The animals were fed with a folate-deficient rodent diet (Harlan Laboratories) starting 5 days prior to tumour cell inoculation [15].

SPECT/CT imaging studies

SPECT/CT experiments were performed with a four-head multiplexing multi-pinhole camera (NanoSPECT/CT, Bioscan, Inc., Washington, DC, USA) using collimators of 4×9 holes with a diameter of 1.4 mm. The scans were acquired using Nucline software (version 1.02, Bioscan, Inc.). Mice were inoculated with KB cells (5×10^6 cells in 100 μl PBS) into the subcutis of each shoulder. Imaging studies were performed about 14 days after KB tumour cell inoculation. SPECT/CT scans were performed the day after intravenous injection of ^{161}Tb-cm09 (~30 MBq, 1 nmol) and ^{177}Lu-cm09 (~30 MBq, 1 nmol) with a time per view of 35 s resulting in a scan time of about 20–30 min. CT scans were performed with the integrated CT using a tube voltage of 55 kVp and an exposure time of 1,000 ms per view. After acquisition, SPECT data were reconstructed iteratively with HiSPECT software (version 1.4.3049, Scivis GmbH) using gamma energies of 47.7 keV (± 10 %) and 74.6 keV (± 10 %) for ^{161}Tb and gamma energies of 56.1 keV (± 10 %), 112.9 keV (± 10 %) and 208.4 keV (± 10 %) for ^{177}Lu. For each gamma line the energy peak had a full width of 20 %. The real-time CT reconstruction used a cone-beam filtered backprojection. SPECT and CT data were automatically coregistered as both modalities share the same axis of rotation. The fused data sets were analysed with the InVivoScope post-processing software (version 2.0, Bioscan, Inc.).

Blood clearance

Two groups of three non-tumour-bearing nude mice were intravenously injected with either ^{161}Tb-cm09 (20 MBq, 1 nmol) or ^{177}Lu-cm09 (20 MBq, 1 nmol). At different time points after injection (5 min, 15 min, 30 min, 1 h, 2 h, 6 h, 20 h, 48 h and 72 h) blood was taken from the tail vein or sublingual vein (3–40 μl) and measured in a gamma counter. The measured radioactivity per millilitre blood was calculated and converted into the percentage of the value measured at the first time point [5 min post-injection (p.i.)] which was set to 100 %.

Biodistribution studies

For post-mortem biodistribution studies mice were inoculated with IGROV-1 cells (6.5×10^6 cells in 100 μl PBS) into the subcutis of each shoulder. The experiments were performed in triplicate approximately 16 days after tumour cell inoculation. The radioconjugates were diluted with PBS to the desired specific activity (2–3 MBq, 0.5 nmol per mouse) for immediate administration via a lateral tail vein. The animals were sacrificed at specified time points between 1 h p.i. and 168 h p.i. and tissues and organs were collected, weighed and counted for radioactivity in a gamma counter. The results were listed as the percentage of the injected dose per gram of tissue weight (%ID/g), using reference counts from a defined volume of the original injectate that was counted at the same time.

To estimate the equivalent absorbed radiation dose for ^{161}Tb-cm09 and ^{177}Lu-cm09 in tumour xenografts and in the kidneys, the following assumptions were made. First, the biodistribution data were considered as equal for ^{161}Tb-cm09 and ^{177}Lu-cm09 and second, the uptake in KB and IGROV-1 tumour xenografts was considered as the same (Supplementary Material).

In vivo therapy studies

Mice were inoculated with KB cells (4.5×10^6 cells in 100 μl PBS) or IGROV-1 cells (7×10^6 cells in 100 μl PBS) under the skin of each shoulder 4 days before the start of therapy at day 0. Mice were weighed 3–4 times a week over a time period of about 7 weeks. Tumour volume was determined every other day using a digital caliper and calculated according to the equation $[0.5\times(L\times W^2)]$ where L is the measurement of the longest axis and W is the measurement of the axis perpendicular to L in millimetres [16]. The relative tumour volume (RTV) was defined as $[V_x/V_0]$ where V_x is the volume in cubic millimetres at a given time x and V_0 at day 0. The efficacy of the folate radioconjugate application was expressed as the percentage tumour growth inhibition (% TGI), calculated using the equation $[100 - (T/C \times 100)]$, where T is the mean RTV of the treated mice and C is the mean RTV in the control group at the time of euthanasia of the first mouse of the control group [17]. Tumour growth delay (TGD_x) was calculated as the time required for the tumour volume to increase x-fold over the initial volume at day 0. Tumour growth delay index ($TGDI_x$) was calculated as the TGD_x ratio of treated over control mice $[TGDI_x=TGD_x(T)/TGD_x(C)]$. For the present studies we calculated the TGD as the time required to observe a fivefold (TGD_5) and tenfold (TGD_{10}) increase of the initial tumour volume allowing the determination of $TGDI_5$ and $TGDI_{10}$.

Endpoint criteria were defined as body weight loss of >15 % of the initial body weight (at day 0), tumour volume >1,500 mm^3 (KB xenografts) or >1,000 mm^3 (IGROV-1 xenografts), ulceration or bleeding of the tumour xenograft or abnormal behaviour indicating pain or unease of the animal. Mice were removed from the study and euthanized upon reaching one of the predefined endpoint criteria. To calculate significance of the survival time or TGD, a *t* test (Microsoft Excel software) was used. All analyses were two-tailed and considered as type 3 (two sample unequal variance). A p value<0.05 was considered statistically significant.

Model 1: ^{161}Tb-cm09 and ^{177}Lu-cm09 therapy in KB tumour-bearing mice Three groups of six mice (group A) or eight mice (groups B and C) were injected with only PBS (group A, control) or with ^{161}Tb-cm09 (group B, 10 MBq, 0.5 nmol) or ^{177}Lu-cm09 (group C, 10 MBq, 0.5 nmol) at day 0 when the average KB tumour volume reached 54±14 mm^3 (group A), 57±17 mm^3 (group B) and 58±16 mm^3 (group C).

Model 2: ^{161}Tb-cm09 and ^{177}Lu-cm09 therapy in IGROV-1 tumour-bearing mice Three groups of six mice (group A) or eight mice (groups B and C) were injected with only PBS (group A, control) or with ^{161}Tb-cm09 (group B, 10 MBq, 0.5 nmol) or ^{177}Lu-cm09 (group C, 10 MBq, 0.5 nmol) at day 0 when the average IGROV-1 tumour volume reached 35±8 mm^3 (group A), 39±13 mm^3 (group B) and 40±12 mm^3 (group C).

Comparison of side effects after therapy with ^{161}Tb-cm09 and ^{177}Lu-cm09 In a separate experiment three groups (A–C) of non-tumour-bearing nude mice were intravenously injected with either only PBS (group A, $n=3$), with 20 MBq ^{161}Tb-cm09 (group B, $n=6$) or ^{177}Lu-cm09 (group C, $n=3$) at day 0. Mice were weighed 3–4 times a week over a time period of 6 months. Plasma parameters including alkaline phosphatase (ALP) and blood urea nitrogen (BUN) were measured from all mice at days 29, 69, 127 and 147 after the start of therapy. Plasma samples were prepared by centrifugation of blood samples (150–200 µl per mouse) drawn from the sublingual vein of each mouse and collected in heparinized vials (Microvette, 200 ml, Sarstedt, Nümbrecht, Germany). For each parameter a plasma volume of 10 µl was required for measurement using a Fuji Dri-Chem 40000i analyser (Polymed Medical Center AG, Glattbrugg, Switzerland).

Results

Radiosynthesis of ^{161}Tb-cm09 and ^{177}Lu-cm09

Radiolabelling of the folate conjugate (cm09) with ^{161}Tb or ^{177}Lu was performed under equal conditions in a solution of sodium acetate and hydrochloric acid at pH 4.5. The radiolabelling was accomplished within 10 min incubation at 95 °C. HPLC-based quality control revealed equal retention times (R_t=19.45 min) for ^{161}Tb-cm09 and ^{177}Lu-cm09. The radiochemical yield of ^{161}Tb-cm09 and ^{177}Lu-cm09 was always >98 % at a specific activity of up to 30 MBq/nmol.

Cell experiments

The viability of KB and IGROV-1 cancer cells was investigated by MTT assays upon exposure of these cells to increasing radioactivity concentrations of ^{161}Tb-cm09 and ^{177}Lu-cm09. Determination of the IC_{50} values—which represent the radioactivity concentration needed to reduce cell viability to 50 % of untreated controls—using KB cells revealed a concentration of 0.014±0.013 MBq/ml for ^{161}Tb-cm09 and 0.063±0.021 MBq/ml for ^{177}Lu-cm09 (Fig. 2a). For IGROV-1 cells an IC_{50} value of 2.53±0.47 MBq/ml was obtained for ^{161}Tb-cm09 and 4.52±0.98 MBq/ml for ^{177}Lu-cm09 (Fig. 2b).

In vivo SPECT/CT imaging studies

In vivo SPECT/CT studies were performed 24 h after injection of ^{161}Tb-cm09 and ^{177}Lu-cm09 in tumour-bearing mice (Fig. 3). High accumulation of radioactivity was found in KB tumour xenografts located on each shoulder and in the kidneys which express the FR in the proximal tubules. Imaging quality was

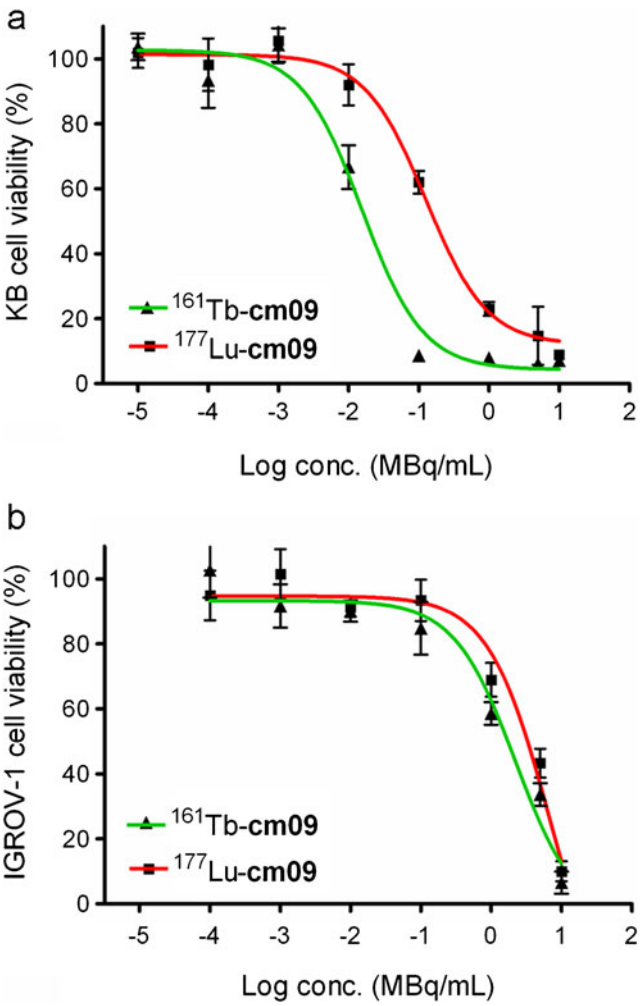

Fig. 2 **a** Inhibitory effects of increasing radioactivity concentrations of ^{161}Tb-cm09 (IC_{50} 0.014±0.013 MBq/ml) and ^{177}Lu-cm09 (IC_{50} 0.063±0.021 MBq/ml) in KB cells. **b** Inhibitory effects of increasing radioactivity concentrations of ^{161}Tb-cm09 (IC_{50} 2.53±0.47 MBq/ml) and ^{177}Lu-cm09 (IC_{50} 4.52±0.98 MBq/ml) in IGROV-1 cells

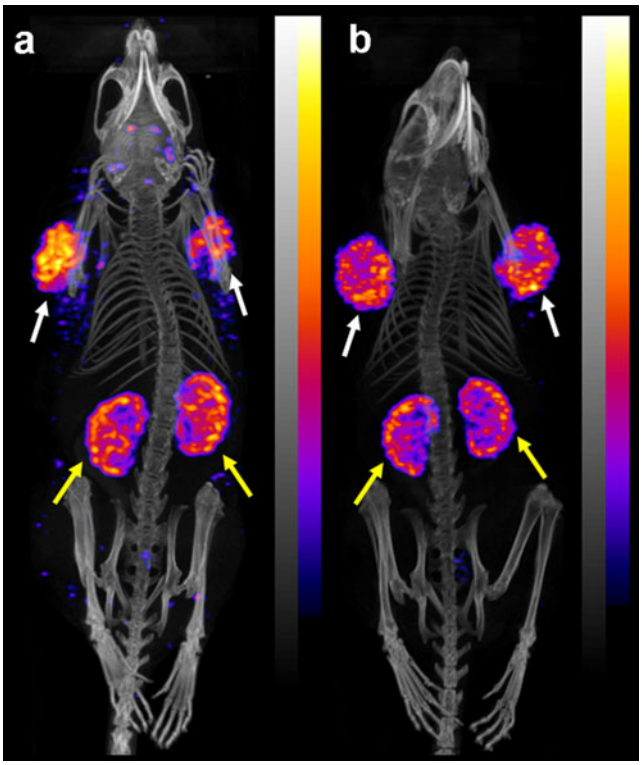

Fig. 3 In vivo SPECT/CT images acquired with dedicated small animal SPECT/CT scanner (NanoSPECT/CT™, Bioscan, Inc., Washington, DC, USA). KB tumour-bearing mice were scanned for 20–30 min 24 h after injection of ~30 MBq ^{161}Tb-cm09 (**a**) and after injection of ~30 MBq ^{177}Lu-cm09 (**b**), respectively. Tumour xenografts and kidneys are indicated with *white* and *yellow arrows*

excellent in the case of a mouse injected with ^{161}Tb-cm09 (Fig. 3a) and comparable to the quality obtained with a mouse which received ^{177}Lu-cm09 (Fig. 3b).

Blood clearance

The results of the study which was performed to determine blood clearance values clearly showed equal clearance curves for ^{161}Tb-cm09 and ^{177}Lu-cm09 over the whole time of investigation (Fig. 4). The average values for ^{161}Tb-cm09 and ^{177}Lu-cm09 did not differ significantly ($p<0.05$). The biological half-life of the radioactive conjugates ^{161}Tb-cm09 and ^{177}Lu-cm09 was about 70 min.

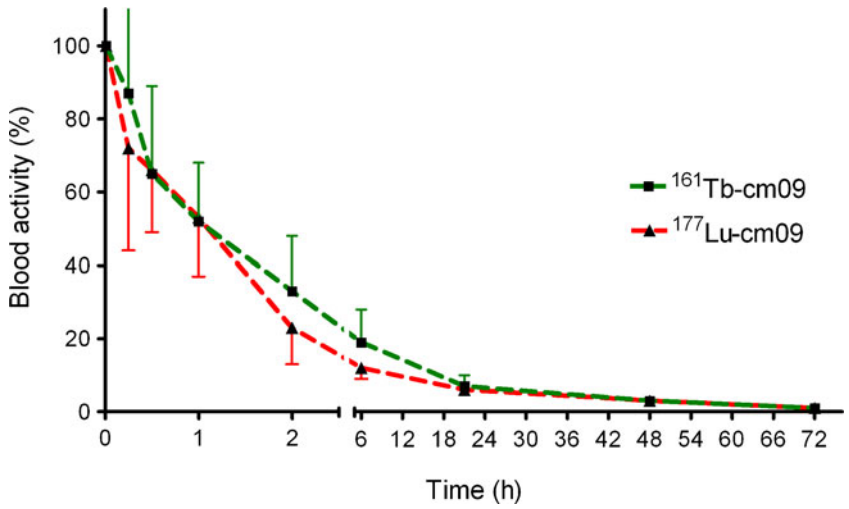

Fig. 4 Blood clearance values for ^{161}Tb-cm09 (*green*) and ^{177}Lu-cm09 (*red*) shown as the blood activity in % of the initially measured radioactivity (5 min p.i. of the radioconjugates) in the blood which was set to 100 %

Biodistribution studies

Biodistribution data of ^{161}Tb-cm09 and ^{177}Lu-cm09 in KB tumour-bearing mice have recently been reported by our group [11, 13]. Herein, additional tissue distribution data were obtained in IGROV-1 tumour-bearing mice after injection of ^{161}Tb-cm09 (Supplementary Material, Table S1). The uptake of ^{161}Tb-cm09 in IGROV-1 tumour xenografts was about 13 %ID/g at 1 h p.i. and 23 %ID/g at 4 and 24 h p.i. Over time, accumulation of radioactivity in the tumour tissue decreased to about 6 %ID/g at 7 day p.i. These findings were equal to those obtained for KB tumour xenografts over the whole time of investigation (Fig. 5, Supplementary Material, Table S2 [11]).

Biological effectiveness of ^{161}Tb-cm09 and ^{177}Lu-cm09

The absorbed fractions for the assumed spherical size of the tumours ranged between 0.90 and 0.95. The calculated absorbed dose of 3.3 Gy/MBq for ^{161}Tb-cm09 and 2.4 Gy/MBq for ^{177}Lu-cm09 in KB and IGROV-1 tumours resulted in an absorbed dose of ~33 Gy and ~24 Gy after injection of 10 MBq ^{161}Tb-cm09 and ^{177}Lu-cm09, respectively. For the kidneys, an absorbed dose of 4.5 Gy/MBq was estimated for ^{161}Tb-cm09 and 3.4 Gy/MBq for ^{177}Lu-cm09. In an additional study non-tumour-bearing mice received 20 MBq ^{161}Tb-cm09 and 20 MBq ^{177}Lu-cm09 resulting in a kidney dose of ~90 Gy for ^{161}Tb-cm09 and ~68 Gy for ^{177}Lu-cm09.

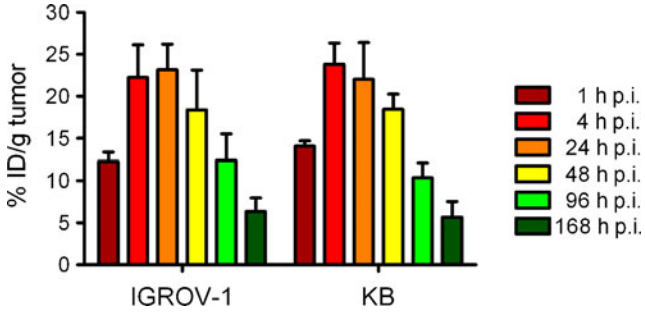

Fig. 5 Accumulation (%ID/g) of ^{161}Tb-cm09 in IGROV-1 and KB tumour xenografts over a time period of 7 days

Therapy studies

The time course of tumour growth in control mice with KB tumours (model 1) was slightly different than in mice bearing IGROV-1 tumours (model 2). While the size of all KB tumours increased uniformly over time, more variability in tumour size and faster tumour growth was observed for IGROV-1 tumour xenografts (Fig. 6a, b). The first control mouse of model 1 had to be euthanized at day 26, whereas in model 2 the first control mouse was euthanized already at day 16, both because of oversized tumours. A clearly reduced tumour growth was found in both groups of mice which received radionuclide therapy, independent of the radioconjugate (^{161}Tb-cm09 versus ^{177}Lu-cm09) and the tumour mouse model (KB versus IGROV-1) (Fig. 6a, b). Consistent in both tumour mouse models was a more pronounced antitumour effect in mice which received ^{161}Tb-cm09 (group B) than in mice which received ^{177}Lu-cm09 (group C). This observation was quantified by calculation of the TGI. In model 1 the TGI was 72 % for mice which received ^{161}Tb-cm09. This value was significantly ($p<0.005$) higher than the TGI of 46 % which was observed in mice treated with ^{177}Lu-cm09. Also, in model 2 the TGI of 90 % for the mice which received ^{161}Tb-cm09 was significantly ($p<0.05$) increased compared to the TGI of 83 % obtained in animals treated with ^{177}Lu-cm09 (Table 2). The TGD indices $TGDI_5$ and $TGDI_{10}$ were increased for mice treated with ^{161}Tb-cm09 compared to mice treated with ^{177}Lu-cm09 in both models (1 and 2, Table 2).

The average survival time in KB tumour-bearing mice (model 1) was 31 days for control mice (group A), 54 days

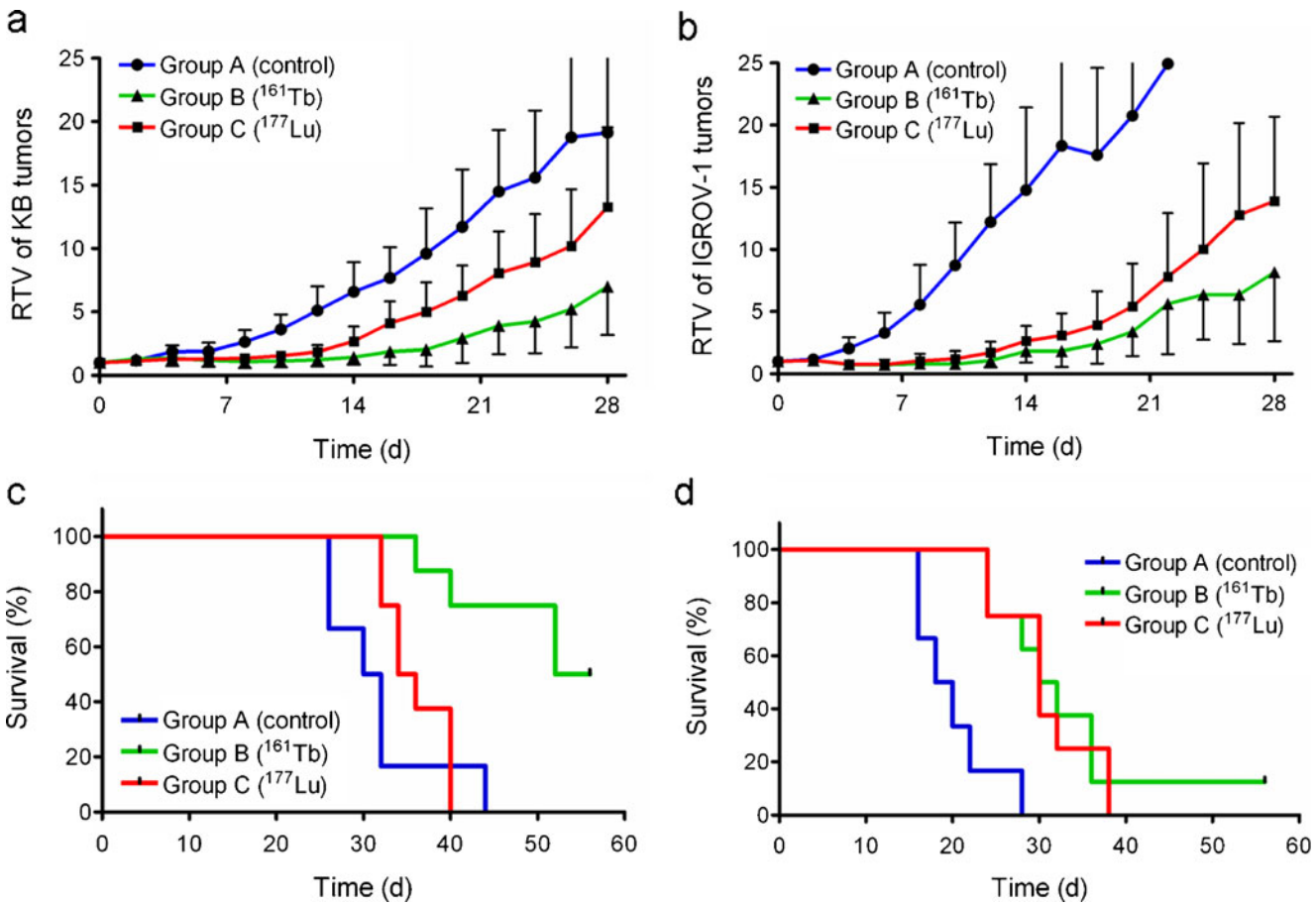

Fig. 6 Tumour growth curves indicated as the relative tumour volumes (*RTV*) of KB tumour-bearing mice (**a**) and IGROV-1 tumour-bearing mice (**b**). Survival curves of KB tumour-bearing mice (**c**) and IGROV-1 tumour-bearing mice (**d**). Control mice (group A) are shown in *blue*, mice treated with ^{161}Tb-cm09 (group B) are shown in *green* and mice treated with ^{177}Lu-cm09 (group C) are shown in *red*

Table 2 Results of the therapy studies using ^{161}Tb-cm09 and ^{177}Lu-cm09 in model 1 and model 2

Model 1: KB tumour-bearing mice							
Group	Mouse ID	Test agent	MBq	$TGDI_5$	$TGDI_{10}$	TGI	Additional survival time
A	A1–A6	PBS	–	1.00	1.00	–	–
B	B1–B8	^{161}Tb-cm09	10	2.17	1.80	72 %	+ 74 %
C	C1–C8	^{177}Lu-cm09	10	1.67	1.30	46 %	+ 13 %
Model 2: IGROV-1 tumour-bearing mice							
Group	Mouse ID	Test agent	MBq	$TGDI_5$	$TGDI_{10}$	TGI	Survival time
A	A1–A6	PBS	–	1.00	1.00	–	–
B	B1–B8	^{161}Tb-cm09	10	2.75	2.67	90 %	+ 63 %
C	C1–C8	^{177}Lu-cm09	10	2.50	2.00	83 %	+ 58 %

for mice treated with ^{161}Tb-cm09 (group B) and 35 days for mice treated with ^{177}Lu-cm09 (group C). In mice with IGROV-1 tumour xenografts (model 2) the average survival time was 19 days for control mice (group A), 31 days for mice treated with ^{161}Tb-cm09 (group B) and 30 days for mice treated with ^{177}Lu-cm09 (group C) (Fig. 6c, d, Table 2).

Comparison of side-effects after therapy with ^{161}Tb-cm09 and ^{177}Lu-cm09

The average value for the two plasma parameters ALP and BUN was in the same range for mice treated with ^{161}Tb-cm09 and ^{177}Lu-cm09 (groups A and B) and control mice (Table 3). Only at day 127 did mice treated with ^{177}Lu-cm09 show an increased value of the ALP level relative to control mice of group A. However, at day 174 the values of the two groups of animals were again in the same range.

During the whole time of investigation plasma parameters such as aspartate aminotransferase, alanine aminotransferase, total bilirubin and albumin of treated mice did not differ significantly from those of control mice (Supplementary Material, Table S3). Moreover, the amount of viable, apoptotic and dead white blood cells were not significantly different among the two groups (B and C) of treated mice and among treated mice and untreated controls (Supplementary Material, Table S4). Investigations of renal uptake of ^{99m}Tc-dimercaptosuccinic acid (DMSA) using quantitative SPECT also did not reveal impairment of kidney function in animals which were treated with ^{161}Tb-cm09 and ^{177}Lu-cm09 (Supplementary Material).

Table 3 List of plasma values of mice of group A ($n=3$), group B ($n=6$) and group C ($n=3$)

Group	Day 29	Day 69	Day 127	Day 174
ALP (U/L)				
A (control)	81±33	51±23	36±10	33±18
B (^{161}Tb-cm09)	57±10	46±14	48±25	49±25
C (^{177}Lu-cm09)	84±8	58±20	64±8*	62±23
BUN (mmol/L)				
A (control)	6.23±0.61	7.27±1.16	6.46±0.29	4.74±0.25
B (^{161}Tb-cm09)	6.21±0.61	7.32±1.11	6.03±1.31	6.68±2.88
C (^{177}Lu-cm09)	6.23±1.59	6.23±0.21	7.53±0.55	7.49±2.30

ALP alkaline phosphatase, *BUN* blood urea nitrogen

*Significance compared to controls ($p<0.05$)

Discussion

In this study ^{161}Tb and ^{177}Lu were compared in vitro and in vivo. Radiolabelling of the DOTA-folate conjugate cm09 was accessible at high specific activity with both radiolanthanides. SPECT phantom studies of ^{161}Tb and ^{177}Lu revealed an excellent imaging quality and a resolution which was comparable for both radionuclides (Supplementary Material, Fig. S1). The quality of the mouse images obtained from in vivo SPECT/CT studies confirmed equal suitability of ^{161}Tb and ^{177}Lu for preclinical imaging purposes. The low-energy gamma rays of ^{161}Tb may be advantageous in view of a clinical application as they result in reduced radiation exposure of non-targeted tissue (e.g. bone marrow) [9, 18]. On the other hand low-energy gamma rays of ^{161}Tb may not be equally appropriate for imaging purposes in patients because of less efficient penetration through the tissue compared to the higher gamma energies of ^{177}Lu (Table 1).

Time-dependent cell uptake and internalization studies confirmed equal in vitro characteristics of ^{161}Tb-cm09 and ^{177}Lu-cm09. In both cell lines we observed largely the same uptake, but in KB cells internalization appeared to be somewhat faster than in IGROV-1 cells (Supplementary Material Fig. S2). In KB and IGROV-1 cells, application of non-internalizing ^{161}Tb and ^{177}Lu (applied as ^{161}Tb- and ^{177}Lu-DTPA complexes) resulted in equal reduction of cell viability (Supplementary Material Fig. S3). However, application of unspecific internalizing ^{161}Tb and ^{177}Lu (applied as $^{161}TbCl_3$ and $^{177}LuCl_3$) resulted consistently in an increased efficacy of ^{161}Tb than of ^{177}Lu (Supplementary Material Fig. S4). As

expected, application of ^{161}Tb-cm09 and ^{177}Lu-cm09 showed an FR-specific inhibitory effect on tumour cell viability in vitro. The inhibitory effect was more pronounced in the case of incubating cells with ^{161}Tb-cm09 than with ^{177}Lu-cm09 and in both cases the effect was clearly better than what was observed with an unspecific treatment (Supplementary Material Fig. S5). In KB cells a 4.5-fold lower radioactivity concentration was required for ^{161}Tb-cm09 to reduce cell viability to 50 % of untreated controls than for ^{177}Lu-cm09. In the case of IGROV-1 cells a 1.8-fold lower radioactivity concentration was required for ^{161}Tb-cm09 to achieve the same effect as with ^{177}Lu-cm09. These in vitro findings were in line with the increased absorbed dose provided by ^{161}Tb (β^--particles, conversion and Auger electrons) compared to ^{177}Lu, if applied at the same radioactivity amount [9, 18].

The in vivo blood clearance curves of ^{161}Tb-cm09 and ^{177}Lu-cm09 demonstrated equal pharmacokinetic properties of these radioconjugates independent of whether they were radiolabelled with ^{161}Tb or ^{177}Lu. Also, both radioconjugates were shown to be stable in vivo, while formation of radioactive metabolites was not observed over at least 2 days after injection (Supplementary Material Fig. S6). The in vivo tissue distribution profile of ^{161}Tb-cm09 and ^{177}Lu-cm09 was equal in both tumour mouse models under standardized experimental conditions. The in vivo studies performed with ^{161}Tb-cm09 revealed an almost equally high uptake (~ 25 %ID/g, 24 h p.i.) in IGROV-1 and KB tumour xenografts (Supplementary Material, Tables S1/S2). Comparison of the in vivo therapy studies in KB and IGROV-1 tumour mouse models showed that the tumour growth was more delayed after application of ^{161}Tb-cm09 than after application of ^{177}Lu-cm09. These findings can be attributed to the fact that the absorbed dose in the tumour tissue was higher for ^{161}Tb-cm09 (3.3 Gy/MBq) than for ^{177}Lu-cm09 (2.4 Gy/MBq). IGROV-1 tumours grew faster than KB tumours but were more sensitive to radionuclide therapy as shown by the tumour growth curves in Fig. 6a, b. However, the difference of the inhibitory effects of ^{161}Tb-cm09 and ^{177}Lu-cm09 on the tumour growth was more pronounced in KB tumours than in IGROV-1 tumours. The reason for this observation is not clear. Since the therapeutic efficacy of conversion and Auger electrons is clearly dependent on the accumulation of the radionuclide in the tumour cell [18–21], it is particularly the internalized fraction of the radioconjugate which would be crucial to benefit from the additional conversion and Auger electrons emitted by ^{161}Tb. Only marginal differences were observed among KB and IGROV-1 cells in terms of the internalized fraction of the radioconjugates in vitro (Supplementary Material, Fig. S2). However, it could be that KB cells internalize the radioconjugates more efficiently in vivo which would explain why the difference among ^{161}Tb-cm09 and ^{177}Lu-cm09 in terms of TGD was greater in KB tumours than in IGROV-1 tumours.

The absorbed dose to the kidneys after application of ^{161}Tb-cm09 (4.5 Gy/MBq) or ^{177}Lu-cm09 (3.4 Gy/MBq) was relatively high. Hence, there was a potential risk of radio-nephrotoxicity. Therefore, an additional in vivo study was performed in which non-tumour-bearing mice received 20 MBq of ^{161}Tb-cm09 and ^{177}Lu-cm09, respectively. This high quantity of radioactivity was chosen because it was known to result in complete tumour regression [13]. Significant alterations of blood plasma parameters were not observed over the whole time period of 6 months. Moreover, SPECT experiments to quantify renal uptake of ^{99m}Tc-DMSA were performed as a measure of kidney function. This method was previously reported by Forrer et al. who investigated kidney damage in rats after PRRT using ^{177}Lu-DOTATATE [22]. Our study revealed similar data for treated animals and untreated control animals independent of whether they received ^{161}Tb-cm09 or ^{177}Lu-cm09 (Supplementary Material Fig. S7, Fig. S8 and Fig. S9). With regard to undesired effects to the kidneys, further studies with a larger cohort of animals per group and variable amounts of injected radioactivity are currently ongoing in our laboratories.

Conclusion

Based on the in vivo studies presented in this work it can be concluded that ^{161}Tb-cm09 provides an enhanced antitumour effect compared to ^{177}Lu-cm09 in KB and IGROV-1 tumour-bearing mice. Radiotoxic side effects were not observed for ^{161}Tb-cm09 and also not for ^{177}Lu-cm09 even at high quantities of injected radioactivity. These data indicate that ^{161}Tb could be a potent alternative to ^{177}Lu for targeted tumour therapy. Further preclinical studies using other tumour-targeting ligands labelled with ^{161}Tb and more detailed investigations about potential radiotoxic side effects are clearly necessary to draw final conclusions about the future clinical perspectives of ^{161}Tb.

Acknowledgments We thank Ulli Köster (Institut Langevin, Grenoble, France) for the target irradiation at ILL and Nadja Romano for technical assistance of the experiments at PSI. This project was financially supported by the Swiss National Science Foundation (Ambizione, Grants PZ00P3_121772 & PZ00P3_138834), COST-BM0607 (C08.0026), the Swiss Cancer League (KLS-02762-02-2011) and the Swiss South African Joint Research Program (JRP 12). Peter Bernhardt was supported by the Swedish National Cancer Society, Swedish Radiation Safety Authority, and the King Gustav V Jubilee Cancer Research Foundation.

Conflicts of interest None.

References

1. Teunissen JJ, Kwekkeboom DJ, Valkema R, Krenning EP. Nuclear medicine techniques for the imaging and treatment of neuroendocrine tumours. Endocr Relat Cancer 2011;18 Suppl 1:S27–51.

2. Teunissen JJ, Kwekkeboom DJ, Krenning EP. Quality of life in patients with gastroenteropancreatic tumors treated with [^{177}Lu-DOTA^{0}, Tyr^{3}]octreotate. J Clin Oncol 2004;22:2724–9.
3. Otte A, Herrmann R, Heppeler A, Behe M, Jermann E, Powell P, et al. Yttrium-90 DOTATOC: first clinical results. Eur J Nucl Med 1999;26:1439–47.
4. Cybulla M, Weiner SM, Otte A. End-stage renal disease after treatment with ^{90}Y-DOTATOC. Eur J Nucl Med 2001;28:1552–4.
5. Rolleman EJ, Melis M, Valkema R, Boerman OC, Krenning EP, de Jong M. Kidney protection during peptide receptor radionuclide therapy with somatostatin analogues. Eur J Nucl Med Mol Imaging 2010;37:1018–31.
6. Kwekkeboom DJ, Bakker WH, Kam BL, Teunissen JJ, Kooij PP, de Herder WW, et al. Treatment of patients with gastro-entero-pancreatic (GEP) tumours with the novel radiolabelled somatostatin analogue [^{177}Lu-DOTA^{0},Tyr^{3}]octreotate. Eur J Nucl Med Mol Imaging 2003;30:417–22.
7. Kwekkeboom DJ, de Herder WW, Kam BL, van Eijck CH, van Essen M, Kooij PP, et al. Treatment with the radiolabeled somatostatin analog [^{177}Lu-DOTA^{0},Tyr^{3}]octreotate: toxicity, efficacy, and survival. J Clin Oncol 2008;26:2124–30.
8. Valkema R, Pauwels SA, Kvols LK, Kwekkeboom DJ, Jamar F, de Jong M, et al. Long-term follow-up of renal function after peptide receptor radiation therapy with ^{90}Y-DOTA^{0},Tyr^{3}-octreotide and ^{177}Lu-DOTA^{0}, Tyr^{3}-octreotate. J Nucl Med 2005;46 Suppl 1:83S–91S.
9. Lehenberger S, Barkhausen C, Cohrs S, Fischer E, Grünberg J, John A, et al. The low-energy β^- and electron emitter ^{161}Tb as an alternative to ^{177}Lu for targeted radionuclide therapy. Nucl Med Biol 2011;38:917–24.
10. de Jong M, Breeman WA, Bernard BF, Rolleman EJ, Hofland LJ, Visser TJ, et al. Evaluation in vitro and in rats of ^{161}Tb-DTPA-octreotide, a somatostatin analogue with potential for intraoperative scanning and radiotherapy. Eur J Nucl Med 1995;22:608–16.
11. Müller C, Zhernosekov K, Köster U, Johnston K, Dorrer H, Hohn A, et al. A unique matched quadruplet of terbium radioisotopes for PET and SPECT and for α- and β-radionuclide therapy: an in vivo proof-of-concept study with a new receptor-targeted folate derivative. J Nucl Med 2012;53:1951–9.
12. Eckerman K, Endo A. ICRP Publication 107. Nuclear decay data for dosimetric calculations. Ann ICRP 2008;38:7–96.
13. Müller C, Struthers H, Winiger C, Zhernosekov K, Schibli R. DOTA conjugate with an albumin-binding entity enables the first folic acid-targeted ^{177}Lu-radionuclide tumor therapy in mice. J Nucl Med 2013;54:124–31.
14. Mosmann T. Rapid colorimetric assay for cellular growth and survival: application to proliferation and cytotoxicity assays. J Immunol Methods 1983;65:55–63.
15. Mathias CJ, Wang S, Lee RJ, Waters DJ, Low PS, Green MA. Tumor-selective radiopharmaceutical targeting via receptor-mediated endocytosis of gallium-67-deferoxamine-folate. J Nucl Med 1996;37:1003–8.
16. Reddy JA, Westrick E, Santhapuram HK, Howard SJ, Miller ML, Vetzel M, et al. Folate receptor-specific antitumor activity of EC131, a folate-maytansinoid conjugate. Cancer Res 2007;67:6376–82.
17. Sanceau J, Poupon MF, Delattre O, Sastre-Garau X, Wietzerbin J. Strong inhibition of Ewing tumor xenograft growth by combination of human interferon-alpha or interferon-beta with ifosfamide. Oncogene 2002;21:7700–9.
18. Bernhardt P, Benjegård SA, Kölby L, Johanson V, Nilsson O, Ahlman H, et al. Dosimetric comparison of radionuclides for therapy of somatostatin receptor-expressing tumors. Int J Radiat Oncol Biol Phys 2001;51:514–24.
19. Capello A, Krenning EP, Breeman WA, Bernard BF, de Jong M. Peptide receptor radionuclide therapy in vitro using [^{111}In-DTPA^{0}]octreotide. J Nucl Med 2003;44:98–104.
20. Ginj M, Hinni K, Tschumi S, Schulz S, Maecke HR. Trifunctional somatostatin-based derivatives designed for targeted radiotherapy using auger electron emitters. J Nucl Med 2005;46:2097–103.
21. Uusijärvi H, Bernhardt P, Ericsson T, Forssell-Aronsson E. Dosimetric characterization of radionuclides for systemic tumor therapy: influence of particle range, photon emission, and subcellular distribution. Med Phys 2006;33:3260–9.
22. Forrer F, Valkema R, Bernard B, Schramm NU, Hoppin JW, Rolleman E, et al. In vivo radionuclide uptake quantification using a multi-pinhole SPECT system to predict renal function in small animals. Eur J Nucl Med Mol Imaging 2006;33:1214–7.
23. Pillai MR, Chakraborty S, Das T, Venkatesh M, Ramamoorthy N. Production logistics of ^{177}Lu for radionuclide therapy. Appl Radiat Isot 2003;59:109–18.
24. Zhernosekov KP, Perego RC, Dvorakova Z, Henkelmann R, Türler A. Target burn-up corrected specific activity of ^{177}Lu produced via ^{176}Lu(n, γ)^{177}Lu nuclear reactions. Appl Radiat Isot 2008;66:1218–20.
25. Lebedev NA, Novgorodov AF, Misiak R, Brockmann J, Rösch F. Radiochemical separation of no-carrier-added ^{177}Lu as produced via the ^{176}Yb(n,γ)^{177}Yb–>^{177}Lu process. Appl Radiat Isotopes 2000;53:421–5.